

1 **Complete protection against SARS-CoV-mediated lethal respiratory disease in aged mice**
2 **by immunization with a mouse adapted virus deleted in E protein**

3

4 Craig Fett¹, Marta L. DeDiego², Jose A. Regla-Nava², Luis Enjuanes², Stanley Perlman^{1*}

5

6 ¹Department of Microbiology, University of Iowa, Iowa City 52242, ²Department of Molecular
7 and Cell Biology, Centro Nacional de Biotecnología (CNB-CSIC), Campus Universidad
8 Autónoma, Darwin 3, Cantoblanco, 28049 Madrid, Spain

9

10 Corresponding author: Stanley Perlman, MD, PhD, Department of Microbiology, BSB 3-712,
11 University of Iowa, IA 52242. Tele: 319-335-8549, Fax 319-335-9006, [Stanley-](mailto:Stanley-perlman@uiowa.edu)
12 perlman@uiowa.edu.

13

14 Running title: Vaccination with mouse adapted SARS-CoV deleted in E

15

16 Word number: Abstract-218

17 Text. 3903

18

19

20 **ABSTRACT**

21

22 Zoonotic coronaviruses, including the one that caused the Severe Acute Respiratory Syndrome
23 (SARS) cause significant morbidity and mortality in humans. No specific therapy for any human
24 coronavirus is available, making vaccine development critical for protection against these
25 viruses. We previously showed that recombinant SARS-CoV (Urbani strain-based) lacking E
26 protein expression (rU- Δ E) provided good but not perfect protection in young mice against
27 challenge with virulent mouse-adapted SARS-CoV (MA15). To improve vaccine efficacy, we
28 developed a second set of E-deleted vaccine candidates, on an MA15 background (rMA15- Δ E).
29 rMA15- Δ E is safe, causing no disease in 6 week, 12 month or 18 month BALB/c mice.
30 Immunization with this virus completely protected mice of three ages from lethal disease and
31 effected more rapid virus clearance. Compared to rU- Δ E, rMA15- Δ E immunization resulted in
32 significantly greater neutralizing antibody and SARS-CoV-specific CD4 and CD8 T cell
33 responses. After challenge, inflammatory cell infiltration, edema and lung destruction were
34 decreased in the lungs of rMA15- Δ E compared to rU- Δ E-immunized 12 month old mice.
35 Collectively, these results show that immunization with a species-adapted attenuated
36 coronavirus lacking E protein expression is safe and provides optimal immunogenicity and long-
37 term protection against challenge with lethal virus. This approach will be generally useful for
38 development of vaccines protective against human coronaviruses as well as against
39 coronaviruses that cause disease in domestic and companion animals.

40

41

42

43 **INTRODUCTION**

44

45 The Severe Acute Respiratory Syndrome (SARS), caused by a novel coronavirus
46 (SARS-CoV), was contracted by approximately 8000 individuals during the 2002-2003
47 epidemic, with a consequent 10% rate of mortality (1, 2). Most strikingly, 50% of patients greater
48 than 60 years of age succumbed to the infection, while no patient less than 24 years died.
49 SARS-CoV has not reappeared in human populations since 2004, but several species of
50 coronaviruses with similarities to SARS-CoV have been identified in bat populations (3-6). A
51 virus (HCoV-EMC) related to two of these bat viruses (BtCoV-HKU4 and BtCoV-HKU5) was
52 recently isolated from several patients in the Middle East who developed severe pneumonia and
53 renal disease (7). How these SARS-like CoV changed host range to infect humans is not known
54 with certainty, but the fact that they did provides the impetus for development of a SARS-CoV
55 vaccine. Most importantly, the development of such a vaccine would provide a guide to rapid
56 engineering and deployment of a vaccine that would be useful against a new, highly pathogenic
57 coronavirus, even if that virus were not SARS-CoV.

58 Several vaccine candidates have been developed since 2003 (8, 9). Anti-virus
59 neutralizing antibodies, which are useful for protecting select populations such as healthcare
60 workers during an outbreak, have been isolated and prepared in large quantities. Several
61 protein subunit vaccines, in which one or more SARS-CoV structural proteins are expressed by
62 a heterologous virus or replicon have also been developed (10). Some of these approaches will
63 be useful in human populations, but the most efficacious vaccines will elicit both antibody and T
64 cell responses directed against the virus. One strategy has been to use non-replicating
65 Venezuelan equine encephalitis replicon particles (VRP) to induce T and B cell responses (11).
66 However, T cell epitopes are located in both the surface glycoproteins and internal proteins
67 such as the nucleocapsid protein (12). An unexpected problem was that VRPs containing only
68 the N or the N and S proteins induce an eosinophilic infiltrate in the lung after challenge with
69 virulent virus, especially in aged mice, making such vaccines not useful (11, 13).

70 Live attenuated vaccines are considered most effective in ability to induce a long-lived
71 balanced immune response. The major problems of using live attenuated vaccines relate to the
72 possibility that viruses may revert to virulence and to the risk that even attenuated live vaccines
73 may cause disease in immunocompromised vaccine recipients. Coronaviruses are well known
74 to recombine (14), so that any attenuated SARS-CoV should be attenuated at several sites to
75 make the probability of reversion as close to nil as possible. Several approaches have been
76 used to minimize the risk of reversion to virulence, including deletion of a minor structural
77 protein, the envelope (E) protein (15-17). In addition to the N and S proteins, all coronaviruses
78 encode at least two additional structural proteins, the E and transmembrane (M) proteins. The E
79 protein is present in the virion in very low amounts and was initially believed to be primarily a
80 structural protein. Subsequent work suggested that E protein was involved in virus assembly
81 and in virus pathogenesis (14). Deletion of the E protein from SARS-CoV impaired replication
82 but did not prevent release of infectious virus, although titers were lower than after infection with
83 E-containing virus (17, 18). Based on these results, we previously developed a recombinant
84 SARS-CoV (human Urbani strain) lacking the E protein (rU- Δ E) and showed that immunization
85 with this virus completely protected hamsters and partially protected mice transgenic for the
86 expression of the SARS-CoV receptor, human angiotensin-converting enzyme 2 (hACE2),
87 against challenge with SARS-CoV (19, 20). hACE2 Tg mice are very sensitive to infection with
88 SARS-CoV, developing an overwhelming encephalitis (21).

89 Human isolates of SARS-CoV, including the Urbani strain, cause no or mild disease in
90 young or aged wild type mice, respectively (22, 23). To analyze the effect of vaccination with E
91 protein-deleted virus in the context of a more severe respiratory infection, we also challenged
92 mice with SARS-CoV that had been adapted to growth in mice by serial passage through
93 BALB/c mice (MA15 strain) (24). MA15 causes severe pneumonia in young BALB/c mice and
94 aged mice of all strains examined (24-26). Immunization of BALB/c mice with rU- Δ E was partly

95 protective against subsequent challenge with MA15, but induced a weak T cell and antibody
96 response (20). Consequently, we have now engineered another virus on an MA15 background
97 (rMA15- Δ E) with the expectation that it will be more immunogenic than rU- Δ E because it is
98 more fit for growth in the mouse lung. We show here that this is indeed the case, with rMA15- Δ E
99 eliciting more potent anti-viral neutralizing antibody and T cell responses than rU- Δ E, but
100 remaining highly attenuated and safe. Further, immunization with rMA15- $\Delta\Delta$ E fully protected 6-
101 10 week, 12 month and 18 month BALB/c mice from challenge with a lethal dose of MA15, and
102 also induced long-term protection.

103

104 **MATERIALS AND METHODS**

105

106 **Mice, virus and cells.** Specific pathogen-free BALB/c mice with ages ranging from 6 weeks to
107 18 months were purchased from the National Cancer Institute. Mice were maintained in the
108 animal care facility at the University of Iowa. All protocols were approved by the University of
109 Iowa Institutional Animal Care and Use Committee. Mouse-adapted SARS-CoV (MA15) (24), a
110 gift from Dr. Kanta Subbarao (National Institutes of Health, Bethesda, Maryland), was grown in
111 Vero E6 cells.

112 **Development of recombinant virus rMA15- Δ E.** Mutations required for mouse adaptation were
113 introduced into the Urbani strain of SARS-CoV using a previously described BAC-based reverse
114 genetics system (27). In specific, mutations were introduced into nsp5 (H133Y, K268N), nsp9
115 (T67A), nsp13 (A4V), S protein (Y436H) and M protein (E11K), resulting in rMA15 (24). All
116 these amino acid substitutions were previously described (24) except for substitution K268N.
117 Introduction of this additional change did not compromise the virulence of MA15 in BALB/c mice
118 (M. L. D, and L. E., unpublished results). Virus deleted in E protein was then generated as
119 previously described (15).

120 **Virus infection and titration.** BALB/c mice were lightly anesthetized with isoflurane and
121 immunized intranasally with 6000 PFU of rMA15-ΔE or PBS. Some mice were then challenged
122 with an intranasal inoculation of 10^5 PFU of MA15 (non recombinant virus). Mice were
123 monitored daily for morbidity and mortality. All work with SARS-CoV was conducted in the
124 University of Iowa Biosafety Level 3 (BSL3) Laboratory. To obtain SARS-CoV titers, lungs were
125 homogenized in phosphate buffered saline (PBS). Virus was titered on Vero E6 cells as
126 previously described (15, 20). Viral titers are expressed as PFU/g tissue for SARS-CoV.

127 **Histology.** Animals were anesthetized and transcardially perfused with PBS followed by zinc
128 formalin. Lungs were removed, fixed in zinc formalin, and paraffin embedded. Sections were
129 stained with hematoxylin and eosin.

130 **Measurement of CD8 and CD4 T cell responses in the lungs.** Mice were sacrificed at the
131 indicated times after infection and single-cell suspensions prepared using Collagenase D
132 (Roche Applied Science, Indianapolis, IN) and 0.1 mg/ml DNase (Roche) to digest the lung (28).
133 Virus-specific CD8 and CD4 T cells were identified by intracellular cytokine staining (ICS) for
134 IFN- γ (28, 29). Briefly, cells were incubated for 5 h with brefeldin A (BD Pharmingen, San Diego,
135 CA) in the presence or absence of SARS-CoV-specific peptides S366 (CD8, HNYKYRYL) or
136 N353 (CD4, VNFNFNGL) (BioSynthesis Inc (Lewisville, TX)). 10^6 cells were then labeled at 4°C
137 for cell surface markers using rat anti-mouse CD4 (RM4-5), rat anti-mouse CD8 α (53-6.7), all
138 from BD Bioscience and rat anti-mouse IFN- γ (XMG1.2) (eBioscience, San Diego). Cells were
139 then fixed/permeabilized with Cytotfix/Cytoperm Solution (BD Biosciences) and labeled with anti-
140 IFN- γ antibody. All flow cytometry data were acquired on a BD FACSCalibur or FACSVerse (BD
141 Biosciences, San Jose, CA) and were analyzed using FlowJo software (Tree Star, Inc.).

142 **Measurement of ELISA titers.** Whole blood was collected and sera prepared. ELISA titers
143 were performed as previously described (20). Briefly, 96-well Maxisorp Immuno Plates (Nunc)
144 were coated with 2×10^5 PFU of formaldehyde and UV-inactivated SARS-CoV (BEI Resources,

145 Manassas, VA). After washing, wells were exposed to threefold dilutions of sera from naïve or
146 immunized mice for 1.5 h. Wells were washed and developed. The ELISA titer was defined as
147 the highest dilution of serum that gave a twofold increase over the background.

148 **Measurement of neutralizing antibody titers.** A virus plaque reduction assay was used to
149 determine serum neutralizing antibody titers (15). Sera were diluted at the indicated ratios and
150 incubated with 50 PFU of MA15 for 30 min. The limit of detection was below 1:30.

151 **Statistical analysis.**

152 A Student's *t* test was used to analyze differences in mean values between groups. All results
153 are expressed as means \pm standard errors of the means (SEM). *P* values of <0.05 were
154 considered statistically significant.

155 **RESULTS.**

156 rMA15- Δ E is safe in 6 week and 12 month BALB/c mice. Previously, we showed that rU- Δ E was
157 attenuated in hamsters, young BALB/c mice and in hACE2-Tg mice, which are highly
158 susceptible to SARS-CoV (15, 17, 19, 20). However, this recombinant virus was constructed on
159 the background of a human coronavirus strain that caused no disease and induced weak anti-
160 virus T cell and antibody responses in in young BALB/c mice (20). Mice, even if aged, develop
161 only mild clinical disease after infection with human-adapted strains (22). By contrast, BALB/c
162 mice of all ages infected with the mouse-adapted MA15 strain develop clinical pneumonia, with
163 more severe disease observed in mice greater than 20 weeks of age (24). To determine
164 whether deletion of the E protein attenuated the MA15 strain, we infected 6 week old BALB/c
165 mice with 5×10^4 PFU of rMA15- Δ E. Mice developed no signs of clinical disease or weight loss,
166 while mice infected with the same dosage of MA15 succumbed to the infection (**Figure 1A,B**).
167 Mice that are 20 weeks of age and older develop more severe disease after infection with MA15
168 (25, 26). To evaluate the safety of rMA15- Δ E in older mice, we infected 12 month old BALB/c

169 mice with the same dosage of rMA15-ΔE. These mice also remained asymptomatic and lost no
170 weight following immunization (**Figure 1C,D**).

171 rMA15-ΔE immunization protects 6 week BALB/c mice from MA15-mediated pulmonary
172 disease. rU-ΔE immunization provides imperfect protection against challenge with MA15 (20)
173 so we assessed efficacy of rMA15-ΔE immunization against challenge with a lethal dose of
174 MA15, comparing it to control (PBS-treated) mice. In preliminary results, we found that
175 intranasal immunization of 6 week BALB/c mice with 3,000-12,000 PFU of rMA15-ΔE resulted in
176 optimal CD4 and CD8 T cell responses at day 7 after immunization; we used 6000 PFU in all
177 subsequent experiments. Intranasal infection of 6 week BALB/c mice with 6000 PFU rMA15-ΔE
178 resulted in a small amount of peribronchial/perivascular inflammatory cell infiltration over the
179 first few days following immunization, as assessed on histological examination (data not
180 shown). Infectious virus was detected at days 2, 4 and 6 after immunization in the lungs of 6
181 week mice immunized with 6000 PFU of rMA15-ΔE, but was no longer detectable by day 8
182 (**Figure 2A**)

183 To evaluate the effect of rMA15-ΔE immunization on clinical disease, we immunized 6
184 week old mice with rMA15-ΔE, rU-ΔE or PBS and then challenged them with 10^5 PFU MA15 at
185 day 21 after immunization. We previously showed that immunization with rU-ΔE resulted in a
186 90% decrease in virus titer compared to PBS by day 5 post challenge (20). rMA15-ΔE
187 immunization was at least as effective, with virus undetectable day 4 after challenge (**Figure**
188 **2B**). All mice in the rMA15-ΔE-treated groups survived and showed no weight loss, while 100%
189 of control mice died (**Figure 2C,D**). In agreement with our previous report, immunization with
190 rU-ΔE protected mice against death although mice showed 10-15% weight loss at early times
191 after infection (20).

192 Immunization with rU- Δ E induced an anti-SARS-CoV T cell response in some but not all
193 mice at day 7 and very low (<1:10) neutralizing antibody titers at day 21 (20). To determine
194 whether the enhanced protection afforded by rMA15- Δ E correlated with greater immunogenicity,
195 we measured anti-viral T cell and antibody responses at days 7 and 21, respectively after
196 immunization. Anti-SARS-CoV neutralizing antibody titers were detectable in 7/9 rMA15- Δ E-
197 immunized mice, with an average titer of $1:95 \pm 21$ (**Figure 2E**). In agreement with our previous
198 report (20), anti-SARS-CoV neutralizing titers were below the limit of detection (1:30) in mice
199 immunized with rU- Δ E.

200 Lung-specific CD4 and CD8 T cell responses were assessed at day 7 after immunization
201 by measuring IFN- γ expression after stimulation with peptides N353 and S366 respectively. As
202 shown in Figure 2F, virus-specific T cell responses were barely detectable in mice inoculated
203 with rU- Δ E. In contrast, approximately $0.4\% \pm 0.1\%$ and $0.8\% \pm 0.1\%$ of the CD4 and CD8 T
204 cells in the lungs of BALB/c mice immunized with rMA15- Δ E were virus-specific.

205 rMA15- Δ E immunization protects 12 month and 18 month BALB/c mice after MA15 challenge.

206 As mice age, they become progressively more susceptible to infection with SARS-CoV, so that
207 12-14 month BALB/c mice develop mild clinical disease and weight loss even after infection with
208 the Urbani strain of SARS-CoV (22). We did not examine the efficacy of rU- Δ E in aged mice in
209 our previous studies. Immunization with 6000 PFU rMA15- Δ E caused no clinical disease in 12
210 month mice (data not shown) and histological examination of immunized lungs revealed a small
211 amount of inflammatory cell infiltration at days 4 and 6 after inoculation (**Figure 3A-C**). Almost
212 no changes were detected in the lungs after immunization with rU- Δ E (**Figure 3D-F**). The
213 kinetics of rMA15- Δ E clearance from the lungs of 12 month mice was delayed compared to
214 rMA15- Δ E-immunized 6 week or rU- Δ E-immunized 12 month mice (compare **Figure 2A and**
215 **4A**), with virus completely cleared by 8 days. This clearance is not due to enhanced replication

216 of rMA15-ΔE in extrapulmonary tissues, since neither rMA15-ΔE or rU-ΔE was detected in the
217 liver, brain or spleen of 12 month old mice at day 2 p.i. (data not shown).

218 Immunization with 6000 PFU of rMA15-ΔE but not PBS or rU-ΔE immunization effected
219 rapid MA15 clearance after challenge with virus largely cleared by day 2 (**Figure 4B**).
220 Immunization with rU-ΔE provided modest protection against lethal disease when 12 month
221 mice were challenged 21 days later (**Figure 4C,D**). In contrast, however, the same dose of
222 rMA15-ΔE completely protected 12 month mice from challenge with 10^5 PFU of MA15.
223 Histological examination of lungs of rU-ΔE or PBS-immunized mice challenged with MA15
224 revealed interstitial and peribronchial/perivascular inflammatory cell infiltration with edema and
225 proteinaceous deposition in airways and alveoli (**Figure 3J-L**) while the lungs of infected
226 rMA15-ΔE-immunized mice showed minimal evidence of lung damage or cellular infiltration
227 (**Figure 3H,I**). In previous vaccine studies, inclusion of the N protein in the immunogen resulted
228 in an eosinophilic infiltration in the lungs on subsequent challenge with SARS-CoV, suggestive
229 of immunopathological disease (11, 13). This was especially evident in aged mice. In contrast,
230 after vaccination with rMA15-ΔE, we did not observe significant eosinophil infiltration into the
231 lungs of 12 month mice after MA15 challenge.

232 Finally, protection correlated with higher anti-virus neutralizing and ELISA antibody titers
233 and CD4 and CD8 T cell responses in rMA15-ΔE compared to rU-ΔE-immunized animals
234 (**Figure 4E-H**). Neutralizing antibody titers were $1:198 \pm 51$ in rMA15-ΔE-immunized mice
235 compared to low titers in 2 mice (1:61) or levels below the limit of detection in six rU-ΔE
236 immunized animals at day 21 after immunization (**Figure 4E**). ELISA titers were low in all mice
237 but significantly higher in rMA15-ΔE-immunized mice compared to those immunized with rU-ΔE
238 (**Figure 4F**). Similarly, N363-specific CD4 and S366-specific CD8 T cell responses were
239 significantly higher in rMA15-ΔE vs rU-immunized mice at day 7 (S366: $4.3 \pm 1.1\%$ vs. 1.0 ± 0.1
240 and N363: $3.7 \pm 0.3\%$ vs 0.03 ± 0.03 , respectively) (**Figure 4G, H**).

241 To determine whether immunization with rMA15- Δ E was safe and protective in even
242 older mice, we immunized 18 month BALB/c mice with 6000 PFU of rMA15- Δ E. Mice showed
243 no signs of clinical disease and minimal weight loss after immunization (**Figure 5A**). Histological
244 examination of the lungs of rMA15- Δ E-immunized mice showed a minor amount of peribronchial
245 and perivascular infiltration (data not shown). Next, we challenged PBS and rMA15- Δ E-
246 immunized 18 month mice with 10^5 PFU of MA15 at 21 days after immunization. Immunization
247 with rMA15- Δ E mice conferred complete protection from lethal disease, with no weight loss
248 observed, while PBS-treated mice developed rapidly fatal disease (**Figure 5B,C**).

249 Prolonged protection against virulent challenge with MA15 after immunization with rMA15- Δ E.

250 Vaccination must result in long-lived protection against challenge with virulent virus to be useful.
251 To begin to address the long term efficacy of rMA15- Δ E immunization against MA15 challenge,
252 we immunized 6 week and 12 month old mice with rMA15- Δ E, rU- Δ E or PBS and then
253 challenged them with 10^5 MA15 at 66 days after immunization. Virus was rapidly cleared from
254 the lungs of 6 week and 12 month rMA15- Δ E-immunized but not from rU- Δ E-immunized or
255 control mice after challenge at day 66 (**Figure 6A,B**). Further, all rMA15- Δ E-immunized, but not
256 rU- Δ E or PBS-treated mice survived subsequent infection with MA15, had no signs of clinical
257 illness and exhibited virtually no weight loss (**Figures 6C-F**). Anti-SARS-CoV antibody titers,
258 whether measured in an ELISA or a plaque reduction neutralization assay were substantially
259 lower in rU- Δ E compared to rMA15- Δ E-immunized mice at day 66 after immunization in both 6
260 week and 12 month mice (**Figures 6G-J**). Notably, neutralizing antibody titers were at or below
261 the limit of detection in both age groups after immunization with rU- Δ E, while titers measured by
262 ELISA were present at low levels in mice immunized at 6 weeks and but were not detected in
263 those immunized at 12 months.

264 Histological examination of the lungs of 12 month mice challenged at day 66 paralleled
265 findings observed in mice infected 21 days after immunization: we detected few changes in the

266 lungs of rMA15- Δ E-immunized mice, with modest amounts of perivascular and peribronchial
267 cellular infiltration and little alveolar or airway edema observed at day 2 or 4 (**Figure 3M,N**). In
268 contrast, after challenge, PBS or rU- Δ E-immunized mice showed airway necrosis and alveolar
269 edema when compared to rMA15- Δ E-immunized mice (**Figure 3O-Q**). Few eosinophils were
270 detected in the inflammatory infiltrate at any time point in any of the mice.

271

272 **DISCUSSION**

273 We showed that immunization of 6 week old BALB/c mice with a recombinant version of
274 a human strain of SARS-CoV lacking E protein expression provided partial protection against
275 challenge with mouse-adapted virus (20). Here, the main objective was to investigate whether
276 adaptation of the virus to the host species in question (mice in this case) would enhance
277 immunogenicity. We show that this in fact occurs since mouse adaptation of the immunizing
278 agent enhances immunogenicity and protection without compromising safety and that long-term
279 protection was induced in 6 week and 12 month old mice. Our results show that mouse
280 adaptation of the E-deleted virus augmented virus replication resulting in detection of infectious
281 rMA15- Δ E in the lungs of 12 month old mice for a modestly longer time post immunization than
282 occurred after rU- Δ E immunization (**Figure 4A**). This delay in virus clearance likely contributed
283 to the development of a more potent anti-viral immune response. This delay in virus clearance
284 may have also contributed to the enhanced anti-virus T cell response observed in 12 month
285 compared to 6 week mice after rMA15- Δ E immunization.

286 Adaptation of zoonotic coronaviruses to efficient growth in human populations generally
287 includes changes in the S glycoprotein that enhance binding to the host cell receptor as well as
288 additional mutations that result in optimal evasion of the innate immune response. The E
289 protein-deleted vaccines that we developed have the potential to be useful against a variety of
290 zoonotic coronaviruses even if these viruses mutate during adaptation since both anti-virus T

291 cell and antibody responses are induced. T cell responses in particular are often induced
292 against internal proteins, such as the nucleocapsid and transmembrane proteins (12), which are
293 less likely to mutate without attenuating the virus. While both anti-virus T cell and antibody
294 responses have been shown to have roles in protection against SARS-CoV, more detailed
295 studies of immune responses in mice infected with the murine coronavirus, mouse hepatitis
296 virus (MHV) demonstrate non overlapping roles for both responses. In the absence of T cells or
297 of either CD4 or CD8 T cells, virus is cleared slowly if at all from infected brains (29-31). On the
298 other hand, initial virus clearance is unaffected by the absence of an antibody response, but
299 virus recrudesces if anti-virus antibodies are not produced locally in the infected brain (32).

300 rMA15-ΔE is very attenuated, causing no clinical disease in BALB/c mice of all ages
301 (**Figures 1 and 5**). However, even with the profound attenuation resulting from the E protein
302 deletion, it will be prudent to introduce additional attenuating mutations into rMA15-ΔE to
303 enhance safety, given the ability of coronaviruses to readily recombine (2, 14). In one approach
304 to developing an attenuated vaccine, the intragenic TRS regions, critical for subgenomic RNA
305 synthesis, were mutated to diminish the possibility that recombination with circulating
306 coronaviruses would occur (16). This virus was also attenuated, which means that introduction
307 of these changes into E protein-deleted virus would enhance safety. Deletion of nsp1, a protein
308 with functions in immune evasion and host cell RNA degradation, is also attenuating (33-35).
309 Deletions in nsp1 have the advantage of being located at a site distant from that of the E
310 protein, making it less likely that recombination with circulating wild type coronaviruses would
311 result in the generation of a virulent virus. Mutations in another nonstructural protein, nsp14 (a
312 3'-5' exonuclease), results in decreased fidelity and virus attenuation *in vivo* (36). Incorporation
313 of mutations in nsp14 into rMA15-ΔE would minimize the risk of reversion.

314 We developed an E protein-deleted virus because previous work suggested that this
315 protein was critical for optimal virus development but was not absolutely required (15, 18). The

316 E protein is a structural protein that is present in the virion in very low amounts (37) and has an
317 important role in virus assembly. Somewhat surprisingly, the requirement for E for the
318 production of infectious virus is not consistent across all coronaviruses. Thus, no infectious virus
319 is released in the absence of E from cells infected with TGEV (38), while virus with an abnormal
320 morphology is released from cells infected with MHV, a betacoronavirus, like SARS-CoV (18). In
321 the case of SARS-CoV, virus shows normal morphology when examined by electron
322 microscopy (15, 17). In addition to its involvement in virion morphogenesis, the E protein also
323 has ion channel activity, although the role of this activity in the virus life cycle is not established
324 (39-41). Recent work has shown that the E protein reduces the stress response in infected cells
325 as well as when introduced exogenously into cells stressed chemically or by infection with a
326 non-coronavirus (42). The E protein also interacts with several host cell proteins and modifies
327 the expression of genes involved in signal transduction, inflammation, apoptosis and the cell
328 cycle, in addition to those related to stress (42). Thus its deletion has multiple effects on the
329 infected cell, potentially attenuating the infection by a variety of mechanisms.

330 Currently, we are identifying domains of E protein responsible for its various roles in
331 assembly, morphogenesis and virulence. Our future efforts at vaccine development will be to
332 maintain some E protein function in order to enhance immunogenicity, while introducing one or
333 more of the changes listed above in order to decrease the likelihood of recombination or
334 reversion to wild type virus.

335

336 **ACKNOWLEDGEMENTS**

337 We thank Drs. Jincun Zhao and Rudragouda Channappanavar for critical review of the
338 manuscript. This work was supported by a grant from the NIH (PO1 AI060699) and from the
339 Ministry of Science and Innovation of Spain (BIO2010-16705) and the European Community
340 project "EMPERIE" (GA223498). JAR was supported by a fellowship from the Fundacion La
341 Caixa.

342

343

REFERENCES

344

345

346

347

348

349

350

351

352

353

354

355

356

357

358

359

360

361

362

363

364

365

366

367

368

369

370

371

372

373

374

375

376

377

378

379

380

381

382

383

384

385

386

387

388

389

1. **Peiris, JS, Guan, Y, and Yuen, KY.** 2004. Severe acute respiratory syndrome. *Nat. Med.* **10**:S88-97.
2. **Perlman, S, and Netland, J.** 2009. Coronaviruses post-SARS: update on replication and pathogenesis. *Nat. Rev. Microbiol.* **7**:439-450.
3. **Hon, CC, Lam, TY, Shi, ZL, Drummond, AJ, Yip, CW, Zeng, F, Lam, PY, and Leung, FC.** 2008. Evidence of the recombinant origin of a bat severe acute respiratory syndrome (SARS)-like coronavirus and its implications on the direct ancestor of SARS coronavirus. *J. Virol.* **82**:1819-1826.
4. **Lau, SK, Li, KS, Huang, Y, Shek, CT, Tse, H, Wang, M, Choi, GK, Xu, H, Lam, CS, Guo, R, Chan, KH, Zheng, BJ, Woo, PC, and Yuen, KY.** 2010. Ecoepidemiology and complete genome comparison of different strains of severe acute respiratory syndrome-related *Rhinolophus* bat coronavirus in China reveal bats as a reservoir for acute, self-limiting infection that allows recombination events. *J. Virol.* **84**:2808-2819.
5. **Lau, SK, Woo, PC, Li, KS, Huang, Y, Tsoi, HW, Wong, BH, Wong, SS, Leung, SY, Chan, KH, and Yuen, KY.** 2005. Severe acute respiratory syndrome coronavirus-like virus in Chinese horseshoe bats. *Proc. Natl. Acad. Sci. (USA)* **102**:14040-14045.
6. **Lau, SK, Woo, PC, Li, KS, Huang, Y, Wang, M, Lam, CS, Xu, H, Guo, R, Chan, KH, Zheng, BJ, and Yuen, KY.** 2007. Complete genome sequence of bat coronavirus HKU2 from Chinese horseshoe bats revealed a much smaller spike gene with a different evolutionary lineage from the rest of the genome. *Virology* **367**:428-439.
7. **Zaki, AM, van Boheemen, S, Bestebroer, TM, Osterhaus, AD, and Fouchier, RA.** 2012. Isolation of a novel coronavirus from a man with pneumonia in Saudi Arabia. *N. Engl. J. Med.* **367**:1814-1820.
8. **Chen, J, and Subbarao, K.** 2007. The Immunobiology of SARS. *Ann. Rev. Immunol.* **25**:443-472.
9. **Enjuanes, L, Dediego, ML, Alvarez, E, Deming, D, Sheahan, T, and Baric, R.** 2008. Vaccines to prevent severe acute respiratory syndrome coronavirus-induced disease. *Virus Res.* **133**:45-62.
10. **Yang, ZY, Werner, HC, Kong, WP, Leung, K, Traggiai, E, Lanzavecchia, A, and Nabel, GJ.** 2005. Evasion of antibody neutralization in emerging severe acute respiratory syndrome coronaviruses. *Proc. Natl. Acad. Sci. (USA)* **102**:797-801.
11. **Deming, D, Sheahan, T, Heise, M, Yount, B, Davis, N, Sims, A, Suthar, M, Harkema, J, Whitmore, A, Pickles, R, West, A, Donaldson, E, Curtis, K, Johnston, R, and Baric, R.** 2006. Vaccine efficacy in senescent mice challenged with recombinant SARS-CoV bearing epidemic and zoonotic spike variants. *PLoS Med.* **3**:e525.
12. **Oh, H-L, Gan, S, Bertoletti, A, and Tan, Y-J.** 2012. Understanding the T cell immune response in SARS coronavirus infection. *Emerg. Microbes Infect.* **1**:e23-e28.
13. **Yasui, F, Kai, C, Kitabatake, M, Inoue, S, Yoneda, M, Yokochi, S, Kase, R, Sekiguchi, S, Morita, K, Hishima, T, Suzuki, H, Karamatsu, K, Yasutomi, Y, Shida, H, Kidokoro, M, Mizuno, K, Matsushima, K, and Kohara, M.** 2008. Prior immunization with severe acute respiratory syndrome (SARS)-associated coronavirus (SARS-CoV) nucleocapsid protein causes severe pneumonia in mice infected with SARS-CoV. *J. Immunol.* **181**:6337-6348.
14. **Masters, PS.** 2006. The molecular biology of coronaviruses. *Adv. Virus Res.* **66**:193-292.

- 390 15. **DeDiego, ML, Alvarez, E, Almazan, F, Rejas, MT, Lamirande, E, Roberts, A, Shieh,**
 391 **WJ, Zaki, SR, Subbarao, K, and Enjuanes, L.** 2007. A severe acute respiratory
 392 syndrome coronavirus that lacks the E gene is attenuated in vitro and in vivo. *J. Virol.*
 393 **81:1701-1713.**
- 394 16. **Yount, B, Roberts, RS, Lindesmith, L, and Baric, RS.** 2006. Rewiring the severe
 395 acute respiratory syndrome coronavirus (SARS-CoV) transcription circuit: Engineering a
 396 recombination-resistant genome. *Proc. Natl. Acad. Sci. (USA)***103:12546-12551.**
- 397 17. **DeDiego, ML, Pewe, L, Alvarez, E, Rejas, MT, Perlman, S, and Enjuanes, L.** 2008.
 398 Pathogenicity of severe acute respiratory coronavirus deletion mutants in hACE-2
 399 transgenic mice. *Virology* **376:379-389.**
- 400 18. **Kuo, L, and Masters, PS.** 2003. The small envelope protein E is not essential for
 401 murine coronavirus replication. *J. Virol.* **77:4597-4608.**
- 402 19. **Lamirande, EW, DeDiego, ML, Roberts, A, Jackson, JP, Alvarez, E, Sheahan, T,**
 403 **Shieh, WJ, Zaki, SR, Baric, R, Enjuanes, L, and Subbarao, K.** 2008. A live attenuated
 404 severe acute respiratory syndrome coronavirus is immunogenic and efficacious in
 405 golden Syrian hamsters. *J. Virol.* **82:7721-7724.**
- 406 20. **Netland, J, DeDiego, ML, Zhao, J, Fett, C, Alvarez, E, Nieto-Torres, JL, Enjuanes, L,**
 407 **and Perlman, S.** 2010. Immunization with an attenuated severe acute respiratory
 408 syndrome coronavirus deleted in E protein protects against lethal respiratory disease.
 409 *Virology* **399:120-128.**
- 410 21. **McCray, PB, Jr., Pewe, L, Wohlford-Lenane, C, Hickey, M, Manzel, L, Shi, L,**
 411 **Netland, J, Jia, HP, Halabi, C, Sigmund, CD, Meyerholz, DK, Kirby, P, Look, DC,**
 412 **and Perlman, S.** 2006. Lethal infection in K18-hACE2 mice infected with SARS-CoV. *J.*
 413 *Virol.* **81:813-821.**
- 414 22. **Roberts, A, Paddock, C, Vogel, L, Butler, E, Zaki, S, and Subbarao, K.** 2005. Aged
 415 BALB/c mice as a model for increased severity of severe acute respiratory syndrome in
 416 elderly humans. *J. Virol.* **79:5833-5838.**
- 417 23. **Subbarao, K, and Roberts, A.** 2006. Is there an ideal animal model for SARS? *Trends*
 418 *Microbiol.* **14:299-303.**
- 419 24. **Roberts, A, Deming, D, Paddock, CD, Cheng, A, Yount, B, Vogel, L, Herman, BD,**
 420 **Sheahan, T, Heise, M, Genrich, GL, Zaki, SR, Baric, R, and Subbarao, K.** 2007. A
 421 mouse-adapted SARS-coronavirus causes disease and mortality in BALB/c mice. *PLoS*
 422 *Pathog.* **3:e5.**
- 423 25. **Sheahan, T, Whitmore, A, Long, K, Ferris, M, Rockx, B, Funkhouser, W,**
 424 **Donaldson, E, Gralinski, L, Collier, M, Heise, M, Davis, N, Johnston, R, and Baric,**
 425 **RS.** 2011. Successful vaccination strategies that protect aged mice from lethal challenge
 426 from influenza virus and heterologous severe acute respiratory syndrome coronavirus. *J.*
 427 *Virol.* **85:217-230.**
- 428 26. **Zhao, J, Zhao, J, Legge, K, and Perlman, S.** 2011. Age-related increases in PGD(2)
 429 expression impair respiratory DC migration, resulting in diminished T cell responses
 430 upon respiratory virus infection in mice. *J. Clin. Invest.* **121:4921-4930.**
- 431 27. **Almazan, F, Dediego, ML, Galan, C, Escors, D, Alvarez, E, Ortego, J, Sola, I,**
 432 **Zuniga, S, Alonso, S, Moreno, JL, Nogales, A, Capiscol, C, and Enjuanes, L.** 2006.
 433 Construction of a severe acute respiratory syndrome coronavirus infectious cDNA clone
 434 and a replicon to study coronavirus RNA synthesis. *J. Virol.* **80:10900-10906.**
- 435 28. **Zhao, J, Zhao, J, Van Rooijen, N, and Perlman, S.** 2009. Evasion by stealth: Inefficient
 436 immune activation underlies poor T cell response and severe disease in SARS-CoV-
 437 infected mice. *PLoS Pathog.* **5:e1000636.**
- 438 29. **Wu, GF, Dandekar, AA, Pewe, L, and Perlman, S.** 2000. CD4 and CD8 T cells have
 439 redundant but not identical roles in virus-induced demyelination. *J. Immunol.* **165:2278-**
 440 **2286.**

- 441 30. **Houtman, JJ, and Fleming, JO.** 1996. Dissociation of demyelination and viral
442 clearance in congenitally immunodeficient mice infected with murine coronavirus JHM. *J.*
443 *Neurovirol.* **2**:101-110.
- 444 31. **Williamson, JS, and Stohlman, SA.** 1990. Effective clearance of mouse hepatitis virus
445 from the central nervous system requires both CD4⁺ and CD8⁺ T cells. *J. Virol.* **64**:4589-
446 4592.
- 447 32. **Ramakrishna, C, Stohlman, SA, Atkinson, RD, Shlomchik, MJ, and Bergmann, CC.**
448 2002. Mechanisms of central nervous system viral persistence: the critical role of
449 antibody and B cells. *J. Immunol.* **168**:1204-1211.
- 450 33. **Kamitani, W, Narayanan, K, Huang, C, Lokugamage, K, Ikegami, T, Ito, N, Kubo, H,**
451 **and Makino, S.** 2006. Severe acute respiratory syndrome coronavirus nsp1 protein
452 suppresses host gene expression by promoting host mRNA degradation. *Proc. Natl.*
453 *Acad. Sci. (USA)* **103**:12885-12890.
- 454 34. **Narayanan, K, Huang, C, Lokugamage, K, Kamitani, W, Ikegami, T, Tseng, CT, and**
455 **Makino, S.** 2008. Severe acute respiratory syndrome coronavirus nsp1 suppresses host
456 gene expression, including that of type I interferon, in infected cells. *J. Virol.* **82**:4471-
457 4479.
- 458 35. **Zust, R, Cervantes-Barragan, L, Kuri, T, Blakqori, G, Weber, F, Ludewig, B, and**
459 **Thiel, V.** 2007. Coronavirus non-structural protein 1 is a major pathogenicity factor:
460 implications for the rational design of coronavirus vaccines. *PLoS Pathog.* **3**:e109.
- 461 36. **Graham, RL, Becker, MM, Eckerle, LD, Bolles, M, Denison, MR, and Baric, RS.**
462 2012. A live, impaired-fidelity coronavirus vaccine protects in an aged,
463 immunocompromised mouse model of lethal disease. *Nat. Med.* **18**:1820-1826.
- 464 37. **Yu, X, Bi, W, Weiss, SR, and Leibowitz, JL.** 1994. Mouse hepatitis virus gene 5b
465 protein is a new virion envelope protein. *Virology* **202**:1018-1023.
- 466 38. **Ortego, J, Ceriani, JE, Patino, C, Plana, J, and Enjuanes, L.** 2007. Absence of E
467 protein arrests transmissible gastroenteritis coronavirus maturation in the secretory
468 pathway. *Virology* **368**:296-308.
- 469 39. **Nieto-Torres, JL, Dediego, ML, Alvarez, E, Jimenez-Guardeno, JM, Regla-Nava, JA,**
470 **Llorente, M, Kremer, L, Shuo, S, and Enjuanes, L.** 2011. Subcellular location and
471 topology of severe acute respiratory syndrome coronavirus envelope protein. *Virology*
472 **415**:69-82.
- 473 40. **Pervushin, K, Tan, E, Parthasarathy, K, Lin, X, Jiang, FL, Yu, D, Vararattanavech,**
474 **A, Soong, TW, Liu, DX, and Torres, J.** 2009. Structure and inhibition of the SARS
475 coronavirus envelope protein ion channel. *PLoS Pathog.* **5**:e1000511.
- 476 41. **Verdia-Baguena, C, Nieto-Torres, JL, Alcaraz, A, DeDiego, ML, Torres, J, Aguilera,**
477 **VM, and Enjuanes, L.** 2012. Coronavirus E protein forms ion channels with functionally
478 and structurally-involved membrane lipids. *Virology* **432**:485-494.
- 479 42. **DeDiego, ML, Nieto-Torres, JL, Jimenez-Guardeno, JM, Regla-Nava, JA, Alvarez, E,**
480 **Oliveros, JC, Zhao, J, Fett, C, Perlman, S, and Enjuanes, L.** 2011. Severe acute
481 respiratory syndrome coronavirus envelope protein regulates cell stress response and
482 apoptosis. *PLoS Pathog.* **7**:e1002315.
- 483
484
485
486

487 **FIGURE CAPTIONS**

488

489

490 Figure 1. Weights and survival in 6 week and 12 month old BALB/c mice after inoculation with

491 5x10⁴ PFU rMA-ΔE. 6 week old (A,B) or 12 month old (C,D) BALB/c mice were inoculated with

492 5x10⁴ PFU of rMA-ΔE or MA15 (non-recombinant) and monitored for weight loss and survival.

493 Data are from 2 independent experiments with 6 mice per group (A,B) or with 9 (rMA-ΔE) or 6

494 (MA15) mice per group (C,D).

495

496 Figure 2. Immunization of 6 week old BALB/c mice with rMA15-ΔE or rU-ΔE and challenge with

497 MA15 at 21 days. 6 week old mice were immunized with 6000 PFU of rMA15-ΔE, rU-ΔE or PBS.

498 (A) Mice were sacrificed at days 2, 4, 6, and 8 post immunization with rMA15-ΔE and virus titers

499 in the lungs measured. (B) rMA15-ΔE-immunized mice were challenged with 10⁵ PFU of MA15

500 at day 21 post immunization and lung virus titers were measured. (C,D) Mice were immunized

501 with rMA15-ΔE, rU-ΔE or PBS and monitored for weight loss and survival. Data are

502 representative of 2 experiments with 4 mice/group (A) or 2 experiments with 4-8 mice/group (B-

503 D). (E) Serum neutralizing antibody titers were measured at day 21 as described in Materials

504 and Methods. (F) Virus-specific CD4 and CD8 T cell responses in the lungs of immunized mice

505 were analyzed by intracellular IFN-γ staining at day 7 as described in Materials and Methods

506 (see Figure 4G,H for representative FACS plots). Average frequency and number of N353-

507 specific CD4 and S366-specific CD8 T cells are shown. Data are representative of one of two

508 independent experiments with 4 mice per group. *p<0.05; **p<0.005; ****p<0.0001.

509

510 Figure 3. Histological changes observed after immunization with rMA-ΔE or rU-ΔE and

511 challenge with MA15. 12 month old BALB/c mice were immunized with 6000 PFU of rMA15-ΔE

512 (A-C), rU-ΔE (D-F), or PBS (G) and sacrificed at days 2, 4 or 6 post immunization. Additional

513 groups of mice were challenged with 10^5 PFU MA15 at days 21 (H-L) and 66 (M-Q) after
514 immunization. Lungs were harvested and processed for histological examination as described in
515 Materials and Methods. Representative images are shown. X-edema, ⊙-cellular debris, ↓
516 denuded epithelium. Original magnification 40X.

517

518 Figure 4. Immunization of 12 month old BALB/c mice with rMA15-ΔE or rU-ΔE and challenge
519 with MA15 at 21 days. (A-D) 12 month old mice were immunized with 6000 PFU of rMA-ΔE, rU-
520 ΔE or PBS. (A) Virus titers at days 2, 4, 6, 8 post immunization. Data are combined results
521 from 2 experiments. (n=4-9 mice/time point/group). (B-D) Mice were challenged at 21 days
522 post immunization with 10^5 PFU of MA15. (B) Virus titers in the lungs were determined at days
523 1, 2 and 4 post challenge (n=4-6 mice/time point/group). (C,D) Mice were monitored for weight
524 loss and survival. Data are representative of 1 of 2 independent experiments with 5-7 mice per
525 group. (E,F) Serum neutralizing and ELISA antibody titers were measured at day 21 after
526 immunization. (G,H) Virus-specific CD4 and CD8 T cell responses were analyzed by
527 intracellular IFN-γ staining as described in Materials and Methods. (Left panels) Representative
528 flow cytometric plots of virus-specific CD4 and CD8 T cells in lungs of 12 month old mice at day
529 7 after immunization. (Right panels) Average frequency and number of N353-specific CD4 and
530 S366-specific CD8 T cells in the lungs of 12 month old mice. Data are representative of one of
531 two independent experiments with 4 mice per group. *p<0.05; **p<0.005; ****p<0.0001.

532

533 Figure 5. Immunization of 18 month old BALB/c mice with rMA15-ΔE and challenge with MA15
534 at 21 days. 18 month old mice were immunized with 6000 pfu of rMA15-ΔE or PBS and
535 monitored for weight loss (A). Twenty one days post immunization, mice were challenged with
536 10^5 PFU of MA15 and monitored for weight loss and survival (B,C). Data are from 2 experiments
537 with 5-6 mice per group.

538 Figure 6. Immunization of 6 week and 12 month old BALB/c mice with rMA15-ΔE or rU-ΔE and
539 challenge with MA15 at 66 days. 6 week old (A,C,E) or 12 month old (B,D,F) mice were
540 immunized with 6000 pfu of rMA15-ΔE, rU-ΔE or PBS and challenged 66 days later with 10⁵
541 MA15. (A,B) Mice were sacrificed for lung virus titers at the times shown post infection (n=3-6
542 mice/group/time) or (C-F) monitored for weight loss and survival (n=5 mice/group). (G-J)
543 Neutralizing and ELISA antibody titers were measured at day 66 after immunization in 6 week
544 (G,H) or 12 month old BALB/c mice. *p<0.05; ***p<0.001; ****p<0.0001.
545

Figure 1. Fett et al.

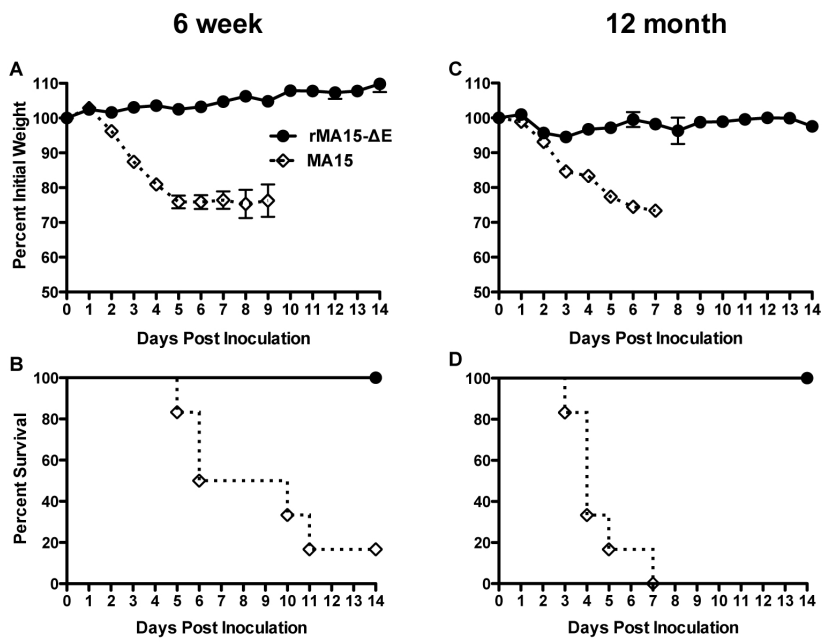


Figure 2. Fett et al.

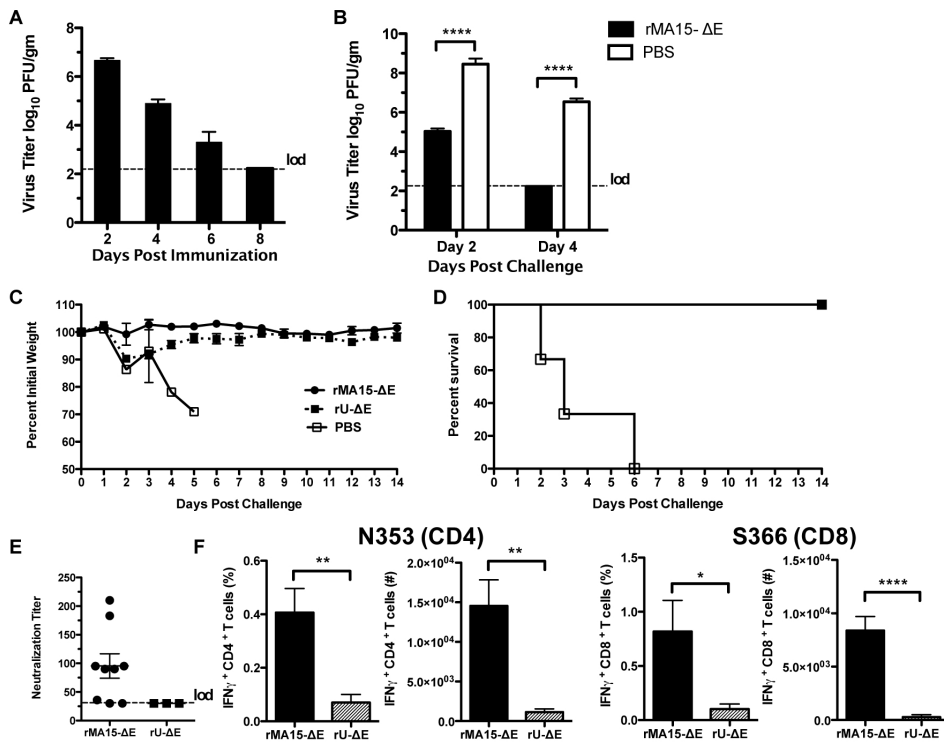


Figure 3. Fett et al.

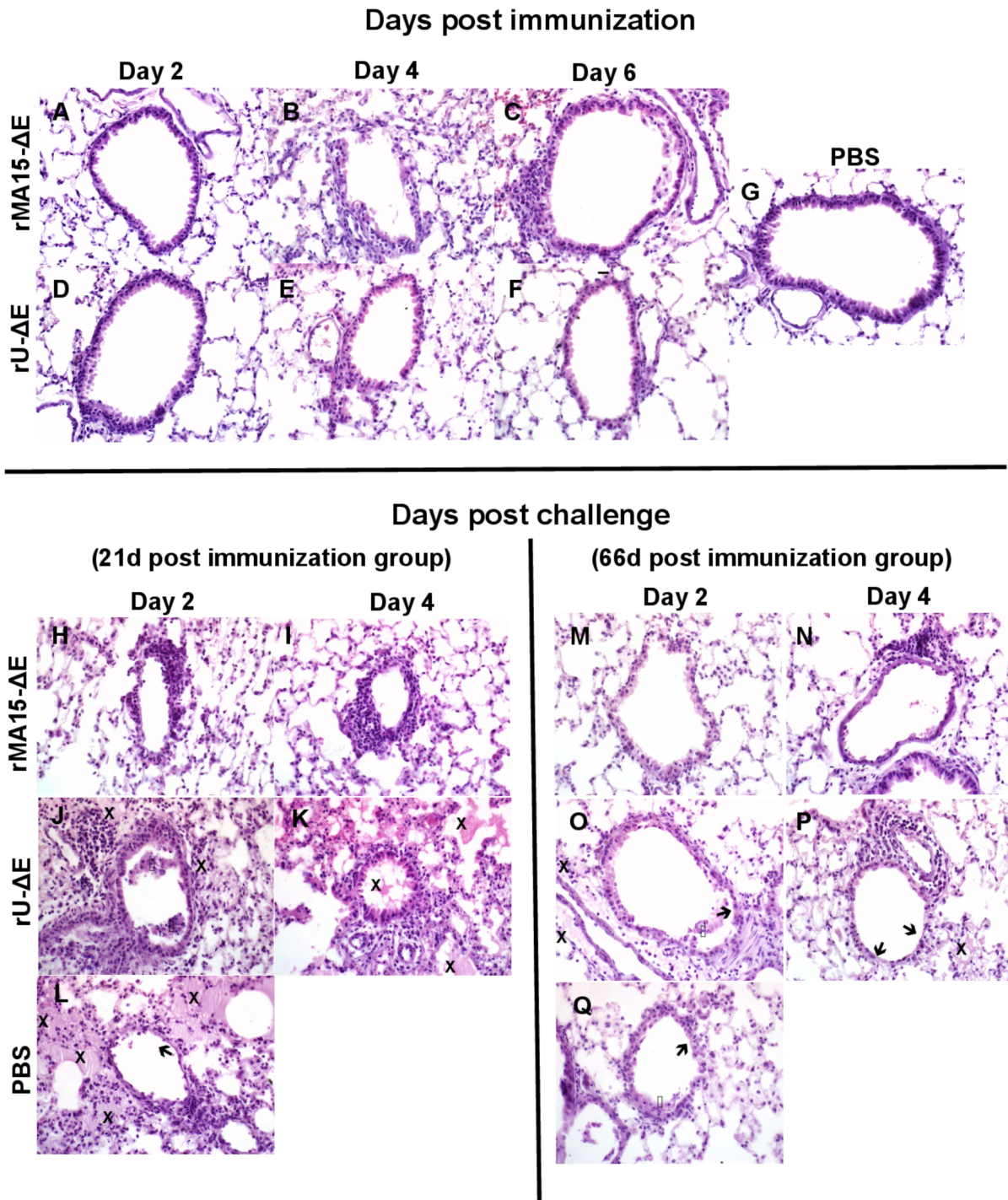


Figure 4. Fett et al.

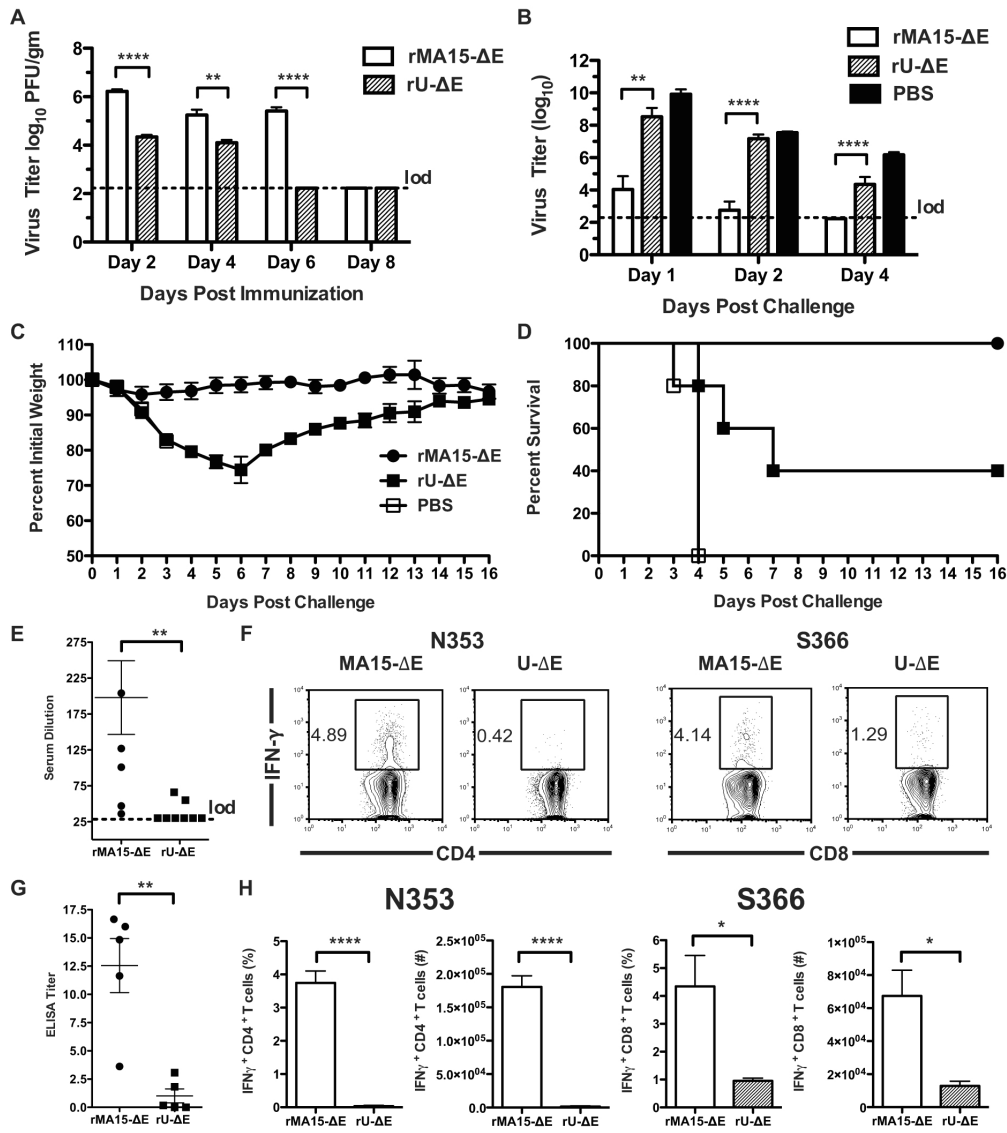


Figure 5. Fett et al.

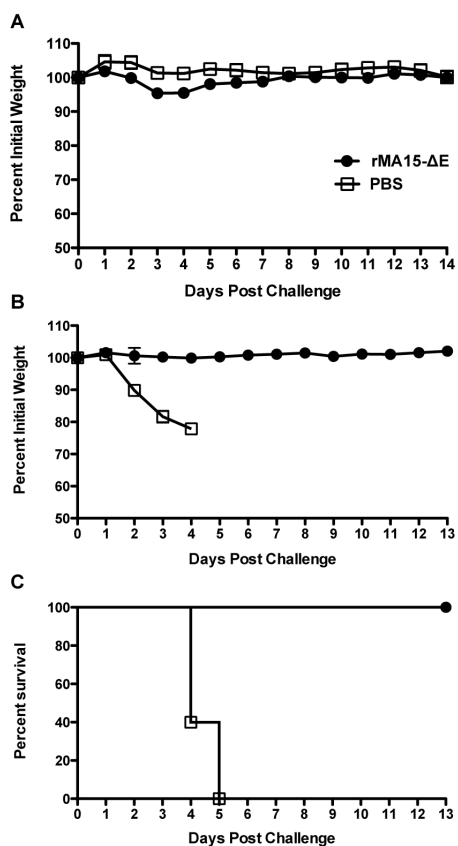


Figure 6. Fett et al.

